JOURNAL OF AIRCRAFT
Vol. 41, No. 3, May–June 2004

Comparison of Residual Strength Estimates for Bolted Lap-Joint Panels

Ala L. Hijazi,* Thomas E. Lacy,† and Bert L. Smith‡
Wichita State University, Wichita, Kansas 67260-0044

Fracture analysis of cracks along mechanically fastened joints is a central issue in the damage tolerance assessment of semimonoque aircraft structures. Nonlinear elastic-plastic finite element analysis, employing the crack-tip-opening-angle criterion, was used to evaluate residual strength of bolted lap-joint 2024-T3 aluminum panels with multiple site damage subjected to Mode-I loading. A total of 36 different crack configurations were analyzed and compared to the experimental results. The effect of different aspects of the finite element modeling procedure on the accuracy of the residual strength predictions was investigated. Modeling of the geometric details of the test panels, such as fasteners and antibuckling restraints, was found to have a considerable effect on the predicted residual strengths. The nonlinear analyses provided reasonable estimates of the residual strength. The numerical results were compared with residual strength predictions obtained from a semi-empirical link-up model. Both approaches were comparable in terms of accuracy when compared to the test data.

Nomenclature

a	=	lead crack half-length
a_n	=	nominal lead crack half-length
c	=	multiple-site-damage (MSD) crack length
D	=	diameter of the fastener hole
e	=	length of lead crack emerging from last hole, $a-(a_n+D/2)$
h_c	=	plane stain core half-height
L	=	ligament length
ℓ	=	half-length of MSD crack and hole, $c+D/2$
β_a	=	geometric correction to stress intensity factor of lead crack
β_ℓ	=	geometric correction to stress intensity factor of the adjacent MSD crack
σ_{LU}	=	residual strength based on Swift link-up model
σ_{STAGS}	=	residual strength predicted by STAGS based on the crack-tip-opening-angle criterion
σ_{Test}	=	residual strength obtained from testing
σ_{WSU2}	=	residual strength based on WSU2 modified link-up model for 2024-T3
σ_{ys}	=	yield strength
Ψ_c	=	critical crack tip opening angle

Introduction

THE aging of aircraft fleets has increased the concern about aircraft structural integrity. As an aircraft is being used beyond its original design life, widespread fatigue damage (WFD) can accumulate at critical locations such as highly loaded fastener holes. The presence of WFD and/or multiple site damage (MSD) can reduce the ability of aircraft structure to carry the design load. Aircraft structures are generally designed to maintain structural integrity in the presence of large (detectable) cracks. However, the presence of an array of small cracks, which might be below detectable limits, can reduce the residual strength of the structure (e.g., skin) below the required level. Thus, methodologies capable of accurately predicting the residual strength of aircraft skins with MSD are desirable. Figure 1 shows a schematic of a panel with MSD.

A variety of analytical and computational approaches can be used to evaluate the residual strength of panels with MSD. Several approaches ranging from simple engineering models to sophisticated computational techniques have been investigated.[1–9] One of the recently used methodologies for residual strength prediction involves use of the crack-tip-opening-angle (CTOA) criterion, or its equivalent the crack-tip-opening-displacement criterion. The CTOA was first identified (in 1961) by Wells[10] as a possible measure of fracture toughness, but it was not until the 1980s that the CTOA criterion was used in elastic-plastic finite element analysis to simulate the fracture behavior of cracked bodies. The past two decades have witnessed a rapid increase in the use of the CTOA criterion in fracture analysis of laboratory specimens as well as full scale structural components. The CTOA criterion can be used to predict tearing initiation, the amount of stable crack growth and the onset of crack instability (i.e., residual strength).[11–13] In the past decade the CTOA criterion has been used to predict the residual strength of aircraft structures with MSD.[2,11] One advantage of the CTOA criterion is that it can be readily used to characterize mixed-mode problems associated with crack face buckling or crack bulging in pressurized structures.[12] A number of two- and three-dimensional elastic-plastic (fracture mechanics oriented) finite element codes exist to facilitate the application of the CTOA criterion.[13] Of course, finite element simulations of complex mechanically fastened joints often require a number of simplifying structural idealizations (implementation of plane strain core concept,[11] use of spring elements to simulate fasteners, etc.) in order to make the problem tractable.

Another approach for evaluating residual strength of skin panels with MSD was introduced by Smith et al.[7] They developed a semi-empirical model (i.e., the WSU2 model) which is a modified version of the Swift link-up model,[6] for predicting residual strength of 2024-T3 aluminum panels with MSD. The WSU2 model was developed using semi-empirical analyses of test data from flat open-hole unstiffened panels with MSD, then was validated using test results of more complex panel configurations.[1,14] A number of similar models were developed by Smith et al.,[7] Broek,[15] and Ingram et al.[16]; however, the WSU2 model was found to yield the most accurate results for a wide range of panel configurations.[1] The WSU2 model was developed to be used with either the A-Basis or the B-Basis yield strength values. The residual (link-up) strength, according to this model, is defined as follows[7]:

$$\sigma_{\mathrm{WSU2}} = \sigma_{\mathrm{LU}}/[C_1\,\ell_n(L) + C_2 + 1] \tag{1}$$

Received 16 January 2003; revision received 3 July 2003; accepted for publication 10 July 2003.

*Postdoctoral Research Fellow, Department of Aerospace Engineering, 1845 Fairmount.

†Assistant Professor, Department of Aerospace Engineering, 1845 Fairmount. Member AIAA.

‡Professor, Department of Aerospace Engineering, 1845 Fairmount. Senior Member AIAA.

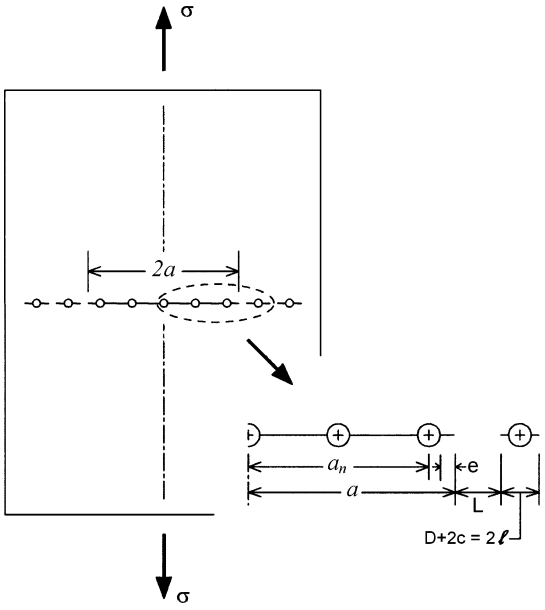

Fig. 1 Schematic diagram of a panel with MSD.

where

$$\sigma_{\mathrm{LU}} = \sigma_{\mathrm{ys}} \sqrt{\frac{2L}{a\beta_a^2 + \ell\beta_\ell^2}} \tag{2}$$

where L, a, and l are shown in Fig. 1. The values of the coefficients are $C_1 = 0.3065$ and $C_2 = 0.3123$ when A-Basis yield strengths σ_{ys} are used in Eq. (2), and $C_1 = 0.3054$ and $C_2 = 0.3502$ when B-Basis yield strengths are used. The stress intensity geometric correction factors (betas) can either be obtained from the literature for simplified configurations[7] or can be determined using finite elements analysis for more complex panel configurations (such as the lap-joint panels considered herein[17]). The basic limitation of the WSU2 model is that it can be only used for Mode-I fracture.

The motivation for this study is to compare residual strength estimates for bolted-joint panels with MSD from the relatively easy to apply WSU2 model to those obtained from somewhat more complex material and geometric nonlinear finite element analysis. Thirty-six single-shear bolted-lap-joint 2024-T3 aluminum panels with different crack configurations were tested to investigate the effect of MSD on the strength of lap-joint panels.[1] Hijazi et al.[17] showed that the WSU2 model was able to predict accurately the residual strength of those panels. In this work the STAGS[18] elastic-plastic finite element code for general shells was used along with the CTOA fracture criterion to predict the residual strength (i.e., the value of remote stress that causes link-up of the lead crack with the adjacent MSD crack) for the 36 crack configurations of the bolted-lap-joint panels. Then residual strength estimates obtained using the WSU2 model and those obtained using finite element simulations were compared to experimental results.

CTOA Fracture Criterion

The CTOA fracture criterion is based on the assumption that crack growth will occur when the angle formed by the upper crack surface, the crack tip, and the lower crack surface, as seen in Fig. 2, reaches a critical value. A fixed distance d of 0.04 in. (1 mm) behind the moving crack tip is typically used to evaluate the value of CTOA.[11] The critical value of CTOA can be obtained experimentally using photographic techniques. Larger CTOA values are observed at crack-growth initiation, then the CTOA decreases and maintains a constant value.[19,20] However, a significant amount of scatter is usually present in the experimental CTOA measurements. More accurate estimates of the critical CTOA angle are obtained by simulating the fracture behavior of laboratory specimens, using elastic-plastic finite element analysis, and determining the angle that best describes the fracture behavior.[11–13,21] Newman et al.[13] showed that a constant

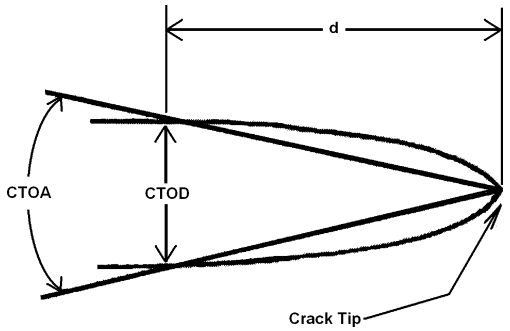

Fig. 2 Definitions of the CTOA and CTOD.

CTOA value can be used to model crack-growth initiation, stable crack growth, and instability for different alloys. Simulating the fracture behavior of cracked panels using the CTOA criterion requires the use of a three-dimensional finite element analysis because of the three-dimensional state of stress at the crack tip.[9] However, two-dimensional plane-stress finite element analysis with a plane-strain core placed at the crack plane (to account for the higher constraint of the crack tip) seems adequate to capture the constraint effects for residual strength predictions.[19] The height of the plane-strain core can influence the accuracy of the analysis. A core height of approximately twice the skin thickness was found to be appropriate for 2024-T3 aluminum.[11] In this study the FRANC3D/STAGS software system was used for modeling and analyzing the bolted-joint panels. FRANC3D[22] is the pre/postprocessor, whereas STAGS[18] is used in performing the nonlinear elastic-plastic thin-shell finite element analysis.

Test Setup and Data[17]

The test panels were 24 in. wide and constructed with 0.056-in.-thick 2024-T3 clad material, and the load was applied in the transverse-long (T-L) grain orientation (the load perpendicular to the grain). The two sheets of the joint overlapped by 3 in., and were fastened together with three rows of 0.1875-in.-diam steel bolts. The holes were also 0.1875 in. in diameter in an attempt to provide a "neat fit" with no interference, and the nuts were lightly torqued. The bolt pitch, row spacing, and edge distance were 1, 1, and 0.5 in., respectively. Two antibuckling fixtures (consisting of two C channels on both sides of the sheet) were placed next to the overlap to prevent out-of-plane movement. The lead crack was centered in the middle of the panel. The MSD cracks were introduced at the fastener holes adjacent to the lead crack tips. The lead crack and the MSD cracks were cut across the upper row of fasteners of the outer sheet. The cracks were produced using a 0.06-in.-thick jeweler's saw. Figure 3 shows a schematic diagram of the test panels. A total of 36 panels with different crack configurations were tested. Nine out of the 36 configurations did not have MSD cracks at the adjacent fastener hole. Tests were performed under displacement control to prevent total failure of the panel and were terminated after the first link up. Details of the crack configuration and the value of remote stress producing link up (i.e., residual strength σ_{Test}) for each of the 36 panels are given in Table 1. Residual strength is defined herein as the value of remote stress at which the ligament between the lead crack and the adjacent MSD crack, or fastener hole, failed. Previous testing demonstrated that there was relatively insignificant scatter in the measured residual strengths.[1] Hence, no duplicate specimens were considered here.

Finite Element Modeling Procedure

The lap-joint sheets were modeled with quadrilateral (Q-4) shell elements with six degrees of freedom per node. The finite element mesh was refined at the crack plane and at the fastener locations (overlap area) to simulate proper load transfer, while the mesh was coarser elsewhere in the model. Quadrilateral (Q-5) shell elements were used to transition between model regions involving different mesh densities. Figure 4 shows a typical finite element mesh of a panel. Plane-stress conditions were assumed everywhere in the

Table 1 Panels test data

Panel ID	$2a_{nom}$, in.	a, in.	e, in.	c, in.	ℓ, in.	L, in.	σ_{Test}, ksi
1	8	4.19375	0.10	0	——	0.7125	20.91
2	8	4.19375	0.10	0.05	0.14375	0.6625	18.38
3	8	4.19375	0.10	0.10	0.19375	0.6125	16.79
4	8	4.24375	0.15	0	——	0.6625	20.02
5	8	4.24375	0.15	0.05	0.14375	0.6125	18.38
6	8	4.24375	0.15	0.10	0.19375	0.5625	16.44
7	8	4.24375	0.15	0.15	0.24375	0.5125	15.45
8	8	4.29375	0.20	0	——	0.6125	19.85
9	8	4.29375	0.20	0.05	0.14375	0.5625	17.38
10	8	4.29375	0.20	0.10	0.19375	0.5125	16.47
11	8	4.29375	0.20	0.15	0.24375	0.4625	15.34
12	8	4.29375	0.20	0.20	0.29375	0.4125	14.72
13	10	5.19375	0.10	0	——	0.7125	17.27
14	10	5.19375	0.10	0.05	0.14375	0.6625	15.56
15	10	5.19375	0.10	0.10	0.19375	0.6125	14.88
16	10	5.24375	0.15	0	——	0.6625	17.17
17	10	5.24375	0.15	0.05	0.14375	0.6125	15.36
18	10	5.24375	0.15	0.10	0.19375	0.5625	14.11
19	10	5.24375	0.15	0.15	0.24375	0.5125	13.10
20	10	5.29375	0.20	0	——	0.6125	16.71
21	10	5.29375	0.20	0.05	0.14375	0.5625	14.82
22	10	5.29375	0.20	0.10	0.19375	0.5125	13.96
23	10	5.29375	0.20	0.15	0.24375	0.4625	12.80
24	10	5.29375	0.20	0.20	0.29375	0.4125	11.88
25	12	6.19375	0.10	0	——	0.7125	14.97
26	12	6.19375	0.10	0.05	0.14375	0.6625	12.95
27	12	6.19375	0.10	0.10	0.19375	0.6125	12.51
28	12	6.24375	0.15	0	——	0.6625	14.78
29	12	6.24375	0.15	0.05	0.14375	0.6125	12.74
30	12	6.24375	0.15	0.10	0.19375	0.5625	11.79
31	12	6.24375	0.15	0.15	0.24375	0.5125	10.88
32	12	6.29375	0.20	0	——	0.6125	14.24
33	12	6.29375	0.20	0.05	0.14375	0.5625	12.25
34	12	6.29375	0.20	0.10	0.19375	0.5125	11.57
35	12	6.29375	0.20	0.15	0.24375	0.4625	10.75
36	12	6.29375	0.20	0.20	0.29375	0.4125	10.04

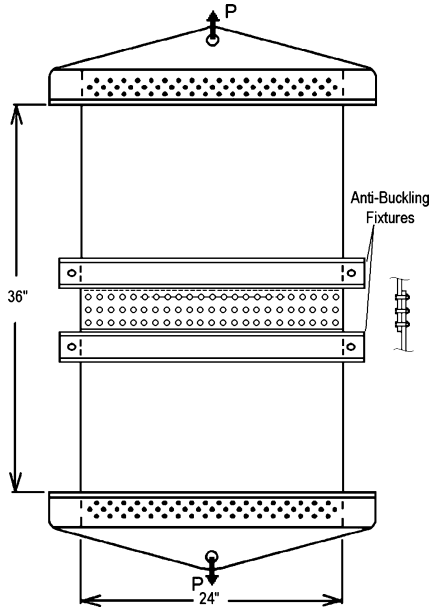

Fig. 3 Front and part-side view schematic of a bolted-lap-joint test panel.

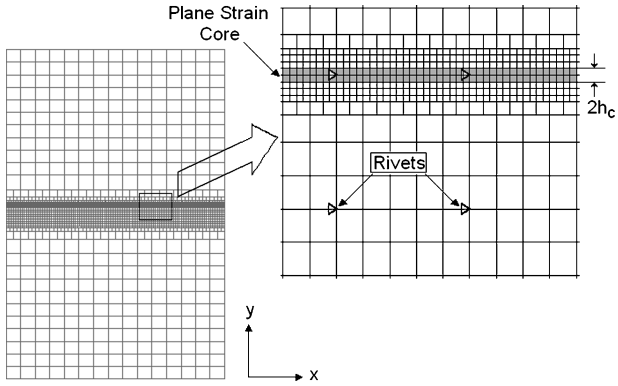

Fig. 4 FRANC3D finite element mesh of the bolted lap-joint panel.

model except for two rows of elements on either side of the crack plane, as shown in Fig. 4. The plane-strain-core elements were included to appropriately account for the added constraint of the crack tips. The height of the plane strain core, $2h_c = 0.1$ in., was equal to almost twice the sheet thickness and corresponded to two rows of elements at the crack plane. The elastic-plastic behavior of the sheet material was accounted for by providing a piecewise linear stress-strain curve.[12] The bottom edge of the model was fixed, and distributed loading was applied to the top edge. A critical CTOA value was specified, and nonlinear analysis was performed to determine the residual strength.

Modeling of Fasteners

Modeling of mechanical fasteners is an important factor for obtaining accurate solutions in fracture analysis, especially when analyzing cracks at fastener holes in mechanically fastened joints. Explicit representation of the fasteners along the crack line (where the fastener shank and the fastener hole are being modeled) is one option for obtaining accurate solutions[23]; however, this capability is not available in FRANC3D. The two sheets were simulated in separate layers, and the fasteners were idealized with two-noded rivet (spring) elements (i.e., the fastener holes were not explicitly modeled). Although it is recognized that such an idealization might not appropriately simulate the stress concentration and stress

redistribution because of the presence of a fastener hole, one goal of this study is to obtain numerical estimates of residual strength using modeling techniques prevalent throughout the literature. Because a number of such studies[2,11,12,24] employ a spring-rivet idealization of mechanical fasteners and do not explicitly model fastener holes, a similar approach was adopted here for comparison purposes. Standard arguments suggest that such a representation might be reasonable, provided that any crack tips of interest are appropriately far removed from such idealized fasteners. The authors do not necessarily advocate such a modeling strategy, but rather wish to compare residual strength estimates from a relatively simple link-up model to those obtained from more complex finite element techniques.

Three rows of two-noded six-degree-of-freedom (three translational and three rotational) rivet elements were used to join the two sheets together. The top row of rivets was attached to the lower surface of the crack only in order to simulate fastener bearing on a single crack face. Elastic properties for the rivets were assumed. Both the fastener and the sheet material properties were accounted for when determining the fastener shearing and bending stiffness.[23] For the 0.1875-in.-diam and 0.112-in.-long steel bolts used to fasten the sheets together, the rivet element properties are bending stiffness $= 1.748\,E6$ lb/in., shear stiffness $= 3.125\,E5$ lb/in., axial stiffness $= 7.149\,E6$ lb/in., and tensional stiffness $= 2.427\,E4$ lb/in. (Ref. 1).

Modeling of Crack Configurations

The 36 crack configurations of the bolted-lap-joint panels were modeled and analyzed. The crack size increment used in the testing (0.05-, 0.1-, 0.15-, and 0.2-in. MSD cracks) necessitated the use of a 0.05-in. element size along the crack plane (the plane strain core) rather than 0.04-in. elements that are commonly used for CTOA analysis.[11] For the configurations with lead crack and MSD cracks, because the holes were not modeled, the fastener-hole diameter was included in the total MSD crack length (the fastener-hole diameter was replaced with four elements totaling 0.2 in.). For the case of no MSD cracks, consistent with Chen,[24] only the lead crack was modeled (i.e., the fastener holes of the adjacent fasteners were ignored). Figure 5 shows a schematic diagram of the crack modeling technique. For the configurations involving a lead crack only, the analyses were stopped when the lead crack tip reached the geometric location of the adjacent fastener hole, which roughly approximates the stress level at which failure of the ligament between the crack tip and the hole occurred.

Critical CTOA (Ψ_c) Value

A critical CTOA value Ψ_c is used in the analysis to simulate the onset of crack-growth initiation and tearing process. STAGS employs a nodal release algorithm to simulate elastic-plastic crack growth along a predetermined path. At each load increment the CTOA is evaluated. When the opening angle reaches the critical

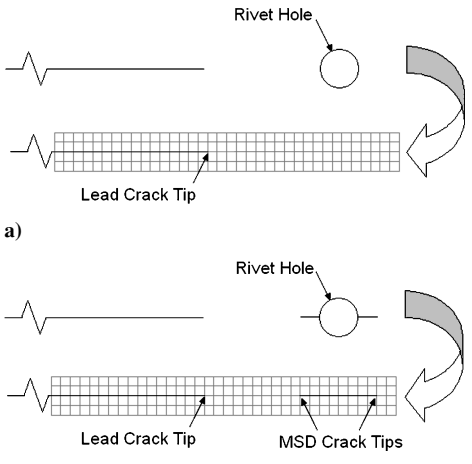

Fig. 5 Schematic of the crack modeling procedure: a) lead crack only and b) lead crack and MSD.

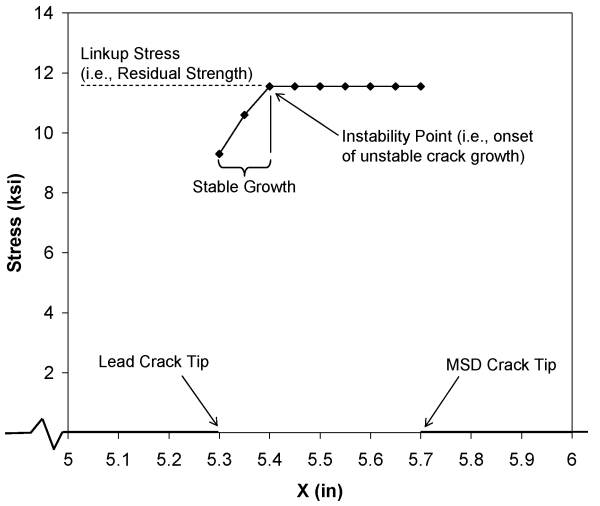

Fig. 6 Crack tearing process for one of the lead crack and MSD configurations from STAGS analysis.

value, the crack tip node is released, and the crack advances to the next node. This process continues until the crack tip reaches a predefined end node or adjacent crack tips meet for the MSD case. In this study crack growth was governed by monitoring the critical CTOA Ψ_c at a distance of one element length (0.05 in.) behind each crack tip. For crack growth under load control conditions, the applied load will generally increase until it reaches a constant value that defines the residual strength (i.e., the growth becomes unstable). This can be seen in Fig. 6, where the applied stress vs crack extension curve for one of the MSD configurations is shown.

There are no standard values of the critical CTOA for aluminum alloys. Experimental measurements of the critical CTOA for thin-sheet aluminum alloys are not very accurate. In addition, a significant amount of scatter (± 1 deg) is always present in the experimental measurements.[8,12,19,20,25] Numerical simulation of test specimens is usually used to determine a critical CTOA value that fits the residual strength and crack growth observed in testing.[8,11–13,21,25,26] Such finite element simulations usually result in estimated CTOA values different than the experimentally measured values but within the scatter band.[8,11,12] Sutton et al.[20] reported an experimentally measured value of $\Psi_c = 4.7$ deg for 2024-T3 aluminum in the T-L grain direction. This value was first used for nine of the crack configurations and was found to cause the analysis to overpredict the test results. A critical CTOA value of $\Psi_c = 4.2$ deg was found to fit the measured residual strengths much better. Table 2 shows the experimental residual strength results for the nine crack configurations and the predicted residual strengths obtained using $\Psi_c = 4.2$ and 4.7 respectively along with the errors for each (where the error is defied as the absolute value of the percent difference between test value and the predicted residual strength value).

In Fig. 7 the STAGS residual strength predictions are plotted vs the corresponding test values. Points lying along the 45-deg line mean that the predicted value and the test value are equal, which is the case more so for the results obtained using $\Psi_c = 4.2$ deg. Points below the 45-deg line indicate that the predictions were conservative, whereas points above that 45-deg line indicate that the simulations overpredict the test values. On average, the residual strength predictions based on $\Psi_c = 4.7$ deg were 7% higher than those obtained using $\Psi_c = 4.2$ deg.

It should be noted here that a subgroup of the test matrix was used for "tuning" the critical CTOA value. Although typically M(T) or C(T) specimens are used for evaluating the critical CTOA value, the resulting value (4.2 deg) was within the ± 1-deg scatter band of the experimentally measured value (4.7 deg). The reported 4.7-deg value was measured 0.04 in. behind the crack tip for a fatigue-sharpened specimen, whereas the cracks in the bolted-lap-joint panels considered herein were produced using saw cuts, and the critical CTOA value was evaluated 0.05 in. behind the crack tip (i.e., 0.05-in. elements were used at the crack plane in the finite element model).

Table 2 STAGS residual strength predictions using two different Ψ_c values for selected crack configurations (with simulated antibuckling constraints)

Panel ID	σ_{Test}, ksi	$\Psi_c = 4.2$ deg σ_{STAGS}, ksi	$\Psi_c = 4.7$ deg σ_{STAGS}, ksi	$\Psi_c = 4.2$ deg σ_{STAGS}, error, %	$\Psi_c = 4.7$ deg σ_{STAGS}, error, %
3	16.79	18.29	19.55	8.95	16.49
7	15.45	16.89	17.78	9.34	15.07
12	14.72	14.45	16.20	1.83	10.01
15	14.88	14.58	15.44	2.03	3.78
19	13.10	13.25	13.99	1.18	6.83
24	11.88	11.55	12.33	2.78	3.76
27	12.51	12.61	13.14	0.72	4.96
31	10.88	11.23	11.96	3.21	10.01
36	10.04	9.87	10.88	1.72	8.31
——	——	——	——	3.53[a]	8.80[a]

[a]Average error.

Table 3 STAGS residual strength predictions with and without using simulated antibuckling stiffeners for selected crack configurations

		Simulated antibuckling stiffeners?		Simulated antibuckling stiffeners?	
		Yes	No	Yes	No
Panel ID	σ_{Test}, ksi	σ_{STAGS}, ksi	σ_{STAGS}, ksi	σ_{STAGS}, error,%	σ_{STAGS}, error, %
3	16.79	18.29	14.72	8.95	12.33
7	15.45	16.89	13.09	9.34	15.25
12	14.72	14.45	11.82	1.83	19.70
15	14.88	14.58	10.64	2.03	28.52
19	13.10	13.25	9.74	1.18	25.61
24	11.88	11.55	8.68	2.78	26.91
27	12.51	12.61	8.44	0.72	32.55
31	10.88	11.23	7.44	3.21	31.55
36	10.04	9.87	6.89	1.72	31.33
——	——	——	——	3.53[a]	24.86[a]

[a]Average error.

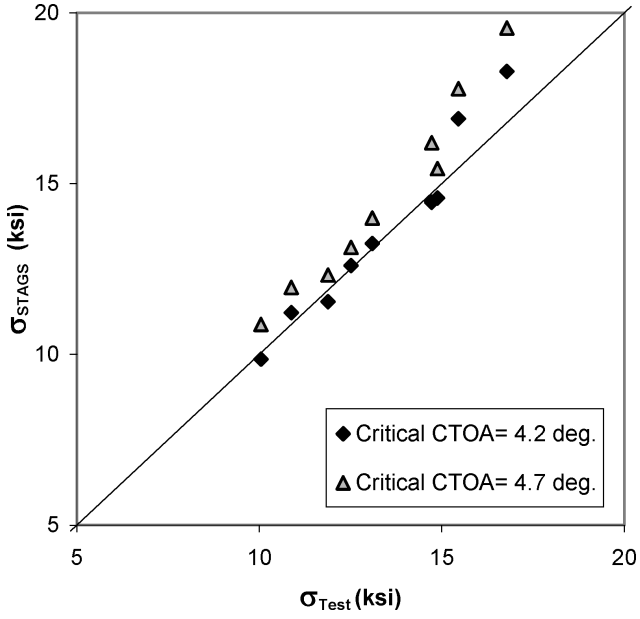

Fig. 7 Test residual strengths compared to STAGS residual strength predictions for two different Ψ_c values.

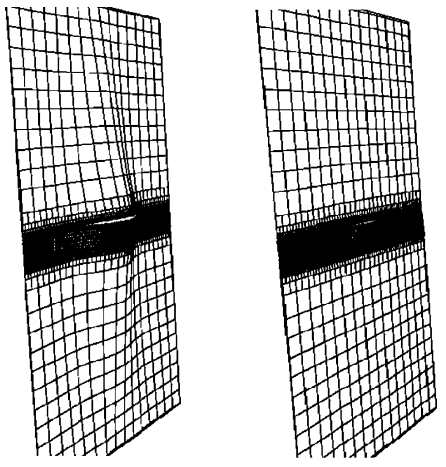

Fig. 8 Effect of the simulated antibuckling stiffeners: a) no antibuckling stiffeners and b) with simulated antibuckling stiffeners.

Modeling of the Antibuckling Stiffeners

Antibuckling stiffeners were used to restrict out-of-plane buckling for all test panels. Also, the fastener heads might have played a role in restricting out-of-plane buckling along the crack faces. The action of the antibuckling stiffeners was simulated in the FRANC3D models by applying a no-rotation line constraint along the overlap edges about an axis parallel to the loading direction (y axis as shown in Fig. 4). Nine crack configurations were analyzed with and without the simulated antibuckling stiffeners to determine the effect they have on the residual strength predictions. Figure 8 shows the deformed mesh for one of the crack configurations with and without the simulated antibuckling stiffeners, where the difference in the amount of out-of-plane buckling is visually apparent. The residual strength estimates of those runs are shown in Table 3 and presented graphically in Fig. 9.

As seen from the results, the antibuckling stiffeners have a noticeable effect on the residual strength predictions. The out-of-plane component of the crack opening displacement for the cases involving no antibuckling constraints resulted in residual strength predictions that, on average, were 26% lower than for the cases involving antibuckling constraints. Figure 10 shows the average difference in residual strength predictions with and without the simulated

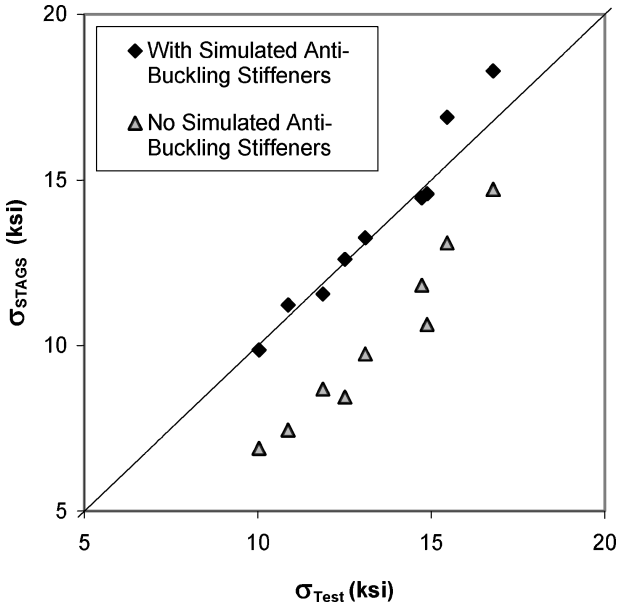

Fig. 9 Test residual strength results compared to STAGS residual strength predictions with and without the simulated antibuckling stiffeners.

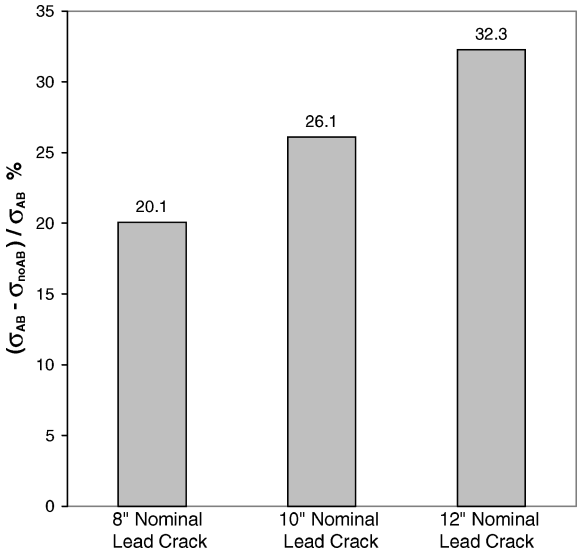

Fig. 10 Effect of lead crack length on STAGS residual strength predictions with and without the simulated antibuckling stiffeners.

antibuckling stiffeners for each of the three nominal lead crack lengths. As can be seen from the figure, the effect of using antibuckling stiffeners on residual strength predictions is more apparent for longer lead cracks.

Results and Discussion

The measured residual strengths and estimated residual strengths obtained using FRANC3D/STAGS as well as the WSU2 model, given in Eq. (1), are summarized in Table 4 for all 36 crack configurations. Note that both estimates resulted in roughly the same average error when compared to experimental results. Figure 11 shows the STAGS and the WSU2 residual strength predictions plotted against the residual strengths obtained from testing. In general, the residual strength predictions obtained from both the STAGS analyses and the WSU2 model correlate reasonably well with the test values. The average error in the WSU2 residual strength predictions for the 36 crack configurations was 4.7%, and the maximum error was 12.3% (Ref. 17). For the STAGS residual strength predictions the average error was 4.8%, and the maximum error was 15.79%. Closer examination of the results obtained by the STAGS

Table 4 STAGS and modified link-up model WSU2 (A-Basis) residual strength predictions for all crack configurations

Panel ID	σ_{Test}, ksi	σ_{STAGS}, ksi	σ_{WSU2}, ksi	σ_{STAGS}, error, %	σ_{WSU2}, error, %
1	20.91	24.09	20.60	15.21	1.47
2	18.38	19.13	17.91	4.09	2.55
3	16.79	18.29	17.12	8.95	1.99
4	20.02	23.18	20.54	15.79	2.59
5	18.38	19.03	17.66	3.55	3.90
6	16.44	17.76	16.83	8.04	2.34
7	15.45	16.89	16.02	9.34	3.66
8	19.85	22.57	20.36	13.73	2.58
9	17.38	18.24	17.35	5.00	0.18
10	16.47	16.88	16.45	2.47	0.11
11	15.34	15.86	15.59	3.37	1.67
12	14.72	14.45	14.68	1.83	0.28
13	17.27	19.21	18.00	11.24	4.25
14	15.56	15.26	15.66	1.96	0.65
15	14.88	14.58	14.98	2.03	0.64
16	17.17	18.75	17.95	9.19	4.54
17	15.36	14.92	15.46	2.91	0.62
18	14.11	14.00	14.77	0.76	4.68
19	13.10	13.25	14.07	1.18	7.42
20	16.71	18.43	17.84	10.29	6.78
21	14.82	14.65	15.18	1.15	2.46
22	13.96	13.70	14.44	1.85	3.44
23	12.80	12.41	13.68	3.02	6.90
24	11.88	11.55	12.87	2.78	8.31
25	14.97	16.07	15.75	7.35	5.25
26	12.95	13.07	13.66	0.89	5.46
27	12.51	12.61	13.08	0.72	4.55
28	14.78	15.64	15.64	5.86	5.85
29	12.74	12.84	13.43	0.78	5.46
30	11.79	12.15	12.84	3.08	8.91
31	10.88	11.23	12.21	3.21	12.31
32	14.24	15.21	15.54	6.77	9.09
33	12.25	12.42	13.20	1.41	7.78
34	11.57	11.52	12.56	0.50	8.51
35	10.75	10.73	11.90	0.18	10.65
36	10.04	9.87	11.20	1.72	11.56
				4.78[a]	4.70[a]

[a]Average error.

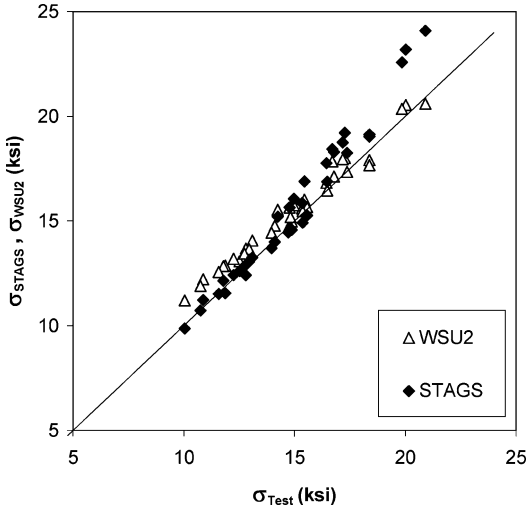

Fig. 11 Residual strength predictions from STAGS analyses and WSU2 model compared to experimental residual strengths.

analyses shows that two factors have influenced the magnitude of the error: the lead crack length and the presence of MSD. Figure 12 shows the effect of the lead crack length on the average error. As can be seen from the figure, the average error decreases with increasing lead crack length. Figure 13 shows the difference in the average error for MSD configurations as opposed to no-MSD configurations for each of the three nominal lead crack lengths as well as for all configurations. Note that for each lead crack length the error in the estimated residual strength was significantly lower for those crack

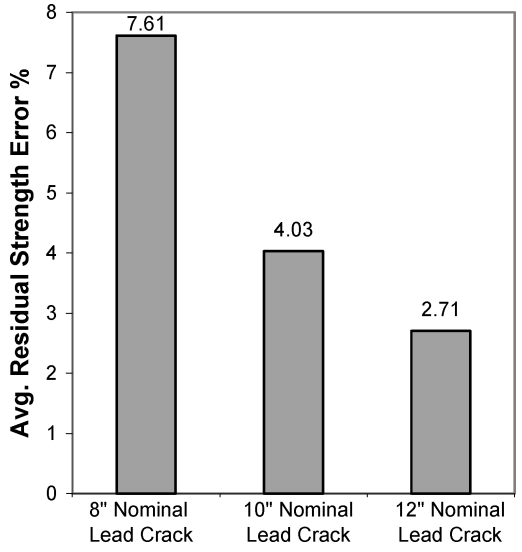

Fig. 12 Effect of lead crack length on the STAGS residual strength predictions error.

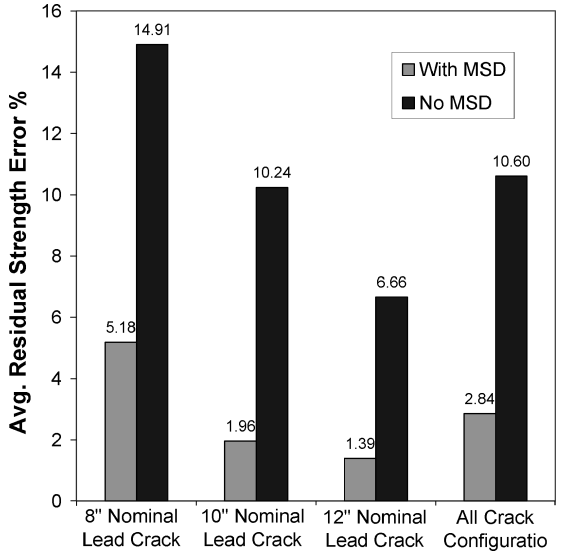

Fig. 13 Effect of the MSD presence on STAGS residual strength predictions error.

configurations with MSD. As seen in Figs. 12 and 13, the average error decreases for longer nominal lead cracks. The error associated with the lead crack length was likely caused by out-of-plane buckling effects. In the test panels both the antibuckling fixtures placed next to the overlap and the bolt heads/nuts along the crack played a role in constraining the out-of-plane bucking. However short-wavelength out-of-plane buckling was observed in the tests. The line constraints used in the finite element model clearly cannot provide the same constraint as in the test panels. Figure 13 shows that the configurations with lead crack only (no MSD) have a significantly larger error than the MSD configurations. The analysis overpredicted failure loads for lead crack only (no-MSD) configurations; this can be expected because the fastener holes were not modeled. The stress concentration caused by the presence of holes has an influence over the amount of lead crack tip plasticity, especially when the crack tip is reasonably close to the edge of the hole. This effect is not accounted for when the holes are not being modeled. This suggests that fastener holes should be accounted for when modeling cracks along a row of fasteners, especially for configurations with no MSD. One possible way to account for the presence of fastener holes for no-MSD cases is to replace the holes by equivalent size cracks that have a critical CTOA Ψ_c value large enough to prevent crack growth from the side of the hole.[8]

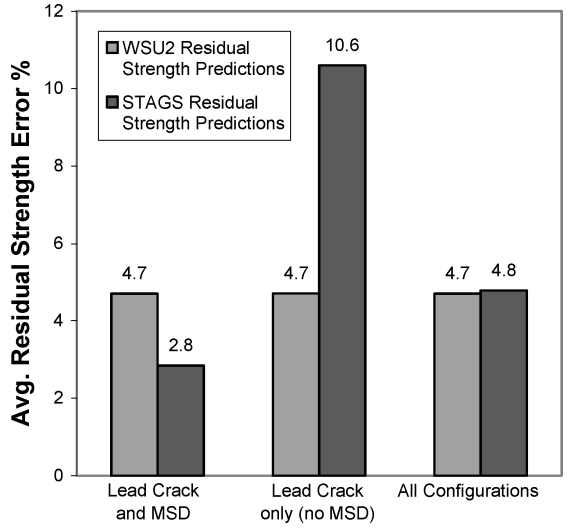

Fig. 14 Comparison between the errors of the modified link-up model WSU2 (A-Basis) and STAGS residual strength predictions.

The results presented herein show that the CTOA criterion gives reasonably good estimates of the residual strength. The average error for all of the 36 crack configurations was 4.8%. The error observed in the residual strength predictions was most likely caused by the modeling assumptions/simplifications. The accuracy of the predicted residual strengths was more sensitive to the modeling of geometric details of the test panels than to the value of the critical CTOA, where a 12% increase in the critical CTOA value resulted in only 7% increase in residual strength, and not accounting for the antibuckling constraints resulted in 26% decrease in residual strength, and not accounting for fastener holes, for no-MSD configurations, resulted in an increase of 8% in the average error.

A comparison of the residual strength predictions obtained by STAGS analyses with those obtained from the modified link-up model WSU2 shows that both are comparable in accuracy with an average error of less than 5% for both. Figure 14 compares the average error in residual strength predictions from both approaches. As seen in the figure, the modified link-up model gave equally accurate predictions for both crack configurations with and without MSD, whereas the STAGS predictions for the no-MSD configurations were not as accurate. The beta factors used in the WSU2 model were determined from finite element simulations of the test panels where the fasteners along the crack line were modeled explicitly.[17]

Conclusions

The CTOA fracture criterion and elastic-plastic finite element code FRANC3D/STAGS were used to predict the residual strength for single-shear bolted-lap-joint 2024-T3 panels with 36 different crack configurations. A constant critical CTOA Ψ_c of 4.2 deg, along with a plane-strain core was used, and STAGS analyses were able to predict the residual strength of the 36 configurations with an average error of less than 5%. The accuracy of this approach was found to be more sensitive to the modeling of geometric details of the test panels than to the value of the critical CTOA. The results presented herein suggest that fastener holes should be accounted for in modeling the configurations with no MSD (lead crack only). Ignoring the fastener holes causes the analysis to overestimate the residual strength.

The residual strength predictions obtained from STAGS analysis were compared with the residual strength predictions obtained from the modified link-up model WSU2 in terms of accuracy. The results from both methods were found comparable with an average error below 5%. This suggests that semi-empirical models, such as the WSU2 model, can efficiently predict residual strength of structures with MSD under Mode-I fracture conditions (given that accurate beta factors are available). Such approaches can serve as an attractive

alternative to large-scale elastic-plastic finite element simulations for predicting residual strength under Mode-I conditions. Extension of the modified link-up approach to the mixed-mode case, however, remains to be fully developed.

Acknowledgments

We acknowledge the support of Kansas National Sciense Foundation (NSF) Cooperative Agreement EPS-9874732 and the Wichita State University High Performance Computing Center.

References

[1]Hijazi, A., "Residual Strength of Thin-Sheet Aluminum Panels with Multiple Site Damage," Ph.D. Dissertation, Dept. of Aerospace Engineering, Wichita State Univ., Wichita, KS, Dec. 2001.

[2]Chen, C., Wawrzynek, P. A., and Ingraffea, A. R., "Residual Strength Prediction of Fuselage Structures with Multiple Site Damage," *Second Joint NASA/FAA/DoD Conference on Aging Aircraft*, NASA CP-1999-208982, Jan. 1999.

[3]Dawicke, D., and Newman, J., Jr., "Evaluation of Various Fracture Parameters for Predictions of Residual Strength in Sheets with Multi-Site Damage," *Proceedings of the First Annual NASA/FAA/DOD Conference on Aging Aircraft*, Ogden, UT, July 1997.

[4]Kuang, J., and Chen, C., "The Failure of Ligaments due to Multiple Site Damage Using Interactions of Dugdale-Type Cracks," *Fatigue and Fracture of Engineering Materials and Structures*, Vol. 21, No. 9, 1998, pp. 1147–1156.

[5]Pidaparti, R., Palakal, M., and Rahman, Z., "Simulation of Structural Integrity Predictions for Panels with Multiple Site Damage," *Advances in Engineering Software*, Vol. 31, No. 2, 2000, pp. 127–135.

[6]Swift, T., "Widespread Fatigue Damage Monitoring Issues and Concerns," *Proceedings of the 5th International Conference on Structural Airworthiness of New and Aging Aircraft*, Hamburg, Germany, June 1993.

[7]Smith, B., Mouak, A., Savill, P., and Myose, R., "Strength of 2024-T3 Aluminum Panels with Multiple Site Damage," *Journal of Aircraft*, Vol. 37, No. 2, 2000, pp. 325–331.

[8]Seshadri, B. R., Newman, J. C., Jr., and Dawicke, D. S., "Residual Strength Analyses of Stiffened and Unstiffened Panels-Part-II: Wide Panels," *Engineering Fracture Mechanics*, Vol. 70, No. 3, 2003, pp. 509–524.

[9]Dawicke, D., and Newman, J., Jr., "Residual Strength Predictions for Multiple Site Damage Cracking Using a Three-Dimensional Finite Element Analysis and a CTOA Criterion," *Fatigue and Fracture Mechanics*, ASTM Special Technical Publ., Vol. 29, No. 1332, 1999, pp. 815–829.

[10]Wells, A., "Application of Fracture Mechanics at and Beyond General Yielding," *British Welding Journal*, Vol. 11, 1961.

[11]Dawicke, D., Newman, J., Jr., Starnes, J., Jr., Rose, C., and Young, R., "Residual Strength Analysis Methodology: Laboratory Coupons to Structural Components," *Proceedings of the Third Joint NASA/FAA/DOD Conference on Aging Aircraft*, Albuquerque, NM, Sept. 1999.

[12]Chen, C., Wawrzynek, P. A., and Ingraffea, A. R., "Residual Strength Prediction of Aircraft Fuselagues Using Crack-Tip Opening Angle Criterion," *Journal of Aircraft*, Vol. 40, No. 3, 2002, pp. 566–575.

[13]Newman, J., James, M., and Zerbst, U., "A Review of the CTOA/CTOD Fracture Criterion," *Engineering Fracture Mechanics*, Vol. 70, Feb.–March 2003, pp. 371–385.

[14]Smith, B., Hijazi, A., and Myose, R., "Summary of the Effect of Multiple Site Damage on the Linkup Strength of 2024-T3 Aluminum Panels," *Proceedings of the Society of Automotive Engineers General Aviation Technology Conference and Exhibition (GATC)*, 2002; also *Journal of Aerospace*, SAE Transactions 2002-01-1534.

[15]Broek, D., "The Effects of Multiple Site Damage on the Arrest Capability of Aircraft Fuselage Structures," *FractuResearch*, TR 9302, Galena, OH, June 1993.

[16]Ingram, J., Kwon, Y., Duffe, K., and Irby, W., "Residual Strength Analysis of Skin Splices with Multiple Site Damage," *The Second Joint NASA/FAA/DOD Conference on Aging Aircraft*, edited by Charles E. Harris, Langley Research Center, Hampton, VA, Jan. 1999, pp. 427–436; also NASA CP-1999-208982.

[17]Hijazi, A., Smith, B., and Lacy, T., "Linkup Strength of 2024-T3 Bolted Lap Joint Panels with Multiple Site Damage," *Journal of Aircraft* (to be published).

[18]Rankin, C., Brogan, F., Loden, W., and Cabiness, H., "STAGS (Structural Analysis of General Shells) Structural Analysis Program," *Version 4.0 User Manual*, Lockheed Martin Advanced Technology Center, Palo Alto, CA, June 2000.

[19]Dawicke, D., Sutton, M., Newman, J., Jr., and Bigelow, C., "Measurement and Analysis of Critical CTOA for an Aluminum Alloy Sheet," NASA CR 109024, NASA Langley Research Center, Hampton, VA, Sept. 1993; also *Fracture Mechanics*, Vol. 25, pp. 358–379.

[20]Sutton, M., Dawicke, D., and Newman, J., Jr., "Orientation Effects on the Measurement and Analysis of Critical CTOA in an Aluminum Sheet," NASA/TM-109153, Sept. 1994; also ASTM Special Technical Publ., No. 1256, Dec. 1995, pp. 243–255.

[21]Dawicke, D., "Residual Strength Predictions Using a Crack Tip Opening Angle Criterion," *FAA-NASA Symposium on the Continued Airworthiness of Aircraft Structure*, DOT/FAA AR-97/2, Vol. II, July 1997, pp. 555–566.

[22]The Cornell Fracture Group, FRANC3D, Version 2, Thin Shell Tutorial Guide, Cornell Univ., Ithaca, NY, URL: www.cfg.cornell.edu.

[23]Cope, D., and Lacy, T., "Modeling Mechanical Fasteners in Lap Joints for Stress Intensity Determination," *Proceedings of the 4th Annual NASA/FAA/DOD Conference on Aging Aircraft*, 2000; also *Collection of Technical Papers—AIAA/ASME/ASCE/AHS/ASC Structures, Structural Dynamics and Materials Conference*, Vol. 1, No. 1, 2002, pp. 274–283.

[24]Chen, C., "Crack Growth Simulation and Residual Strength Prediction in Thin Shell Structures," Ph.D. Dissertation, Dept. of Mechanical Engineering, Cornell Univ., Ithaca, NY, June 1999.

[25]Dawicke, D., and Sutton, M., "CTOA and Crack Tunneling Measurements in Thin Sheet 2024-T3 Aluminum Alloy," *Experimental Mechanics*, Vol. 34, No. 4, 1994, pp. 357–368.

[26]James, M., "A Plane Stress Finite Element Model for Elastic-Plastic Mode I/II Crack Growth," Ph.D. Dissertation, Dept. of Mechanical Engineering, Kansas State Univ., Manhattan, KS, June 1998.